Bioactive Materials 6 (2021) 1628–1638

Contents lists available at ScienceDirect

Bioactive Materials

journal homepage: www.sciencedirect.com/journal/bioactive-materials

Coaxial-printed small-diameter polyelectrolyte-based tubes with an electrostatic self-assembly of heparin and YIGSR peptide for antithrombogenicity and endothelialization

Zhiwen Zeng [a], Chengshen Hu [a,b], Qingfei Liang [a,b], Lan Tang [a,b], Delin Cheng [a,b], Changshun Ruan [a,b,*]

[a] Research Center for Human Tissue and Organs Degeneration, Institute of Biomedicine and Biotechnology, Shenzhen Institutes of Advanced Technology, Chinese Academy of Sciences, Shenzhen, 518055, PR China
[b] University of Chinese Academy of Sciences, Beijing, 100049, PR China

ARTICLE INFO

Keywords:
Coaxial extrusion printing
Electrostatic self-assembly
Sequential release
Antithrombogenicity
Endothelialization

ABSTRACT

Low patency ratio of small-diameter vascular grafts remains a major challenge due to the occurrence of thrombosis formation and intimal hyperplasia after transplantation. Although developing the functional coating with release of bioactive molecules on the surface of small-diameter vascular grafts are reported as an effective strategy to improve their patency ratios, it is still difficult for current functional coatings cooperating with spatiotemporal control of bioactive molecules release to mimic the sequential requirements for antithrombogenicity and endothelialization. Herein, on basis of 3D-printed polyelectrolyte-based vascular grafts, a biologically inspired release system with sequential release in spatiotemporal coordination of dual molecules through an electrostatic self-assembly was first described. A series of tubes with tunable diameters were initially fabricated by a coaxial extrusion printing method with customized nozzles, in which a polyelectrolyte ink containing of ε-polylysine and sodium alginate was used. Further, dual bioactive molecules, heparin with negative charges and Tyr-Ile-Gly-Ser-Arg (YIGSR) peptide with positive charges were layer-by-layer assembled onto the surface of these 3D-printed tubes. Due to the electrostatic interaction, the sequential release of heparin and YIGSR was demonstrated and could construct a dynamic microenvironment that was thus conducive to the antithrombogenicity and endothelialization. This study opens a new avenue to fabricate a small-diameter vascular graft with a biologically inspired release system based on electrostatic interaction, revealing a huge potential for development of small-diameter artificial vascular grafts with good patency.

1. Introduction

Tissue-engineered artificial vessel (TEAV) holds a tremendous promise for the creation of ‘‘replacement vascular’’ with a huge potential for vascular transplantation. With rapid development of new materials and technologies, various tissue-engineered strategies have been devoted to fabricate TEAVs with perfusable structure and suitable performances for vascular regeneration, such as self-assembly, template synthesis, phase separation, wet spinning, electrospinning, three-dimensional (3D) printing and their combination [1,2]. However, there are still few successes in small diameter (≤6 mm) vascular grafts, due to that their small-size structure makes the preparation process difficult and the formation of acute thrombosis and intimal hyperplasia easy after implantation [3].

Recently, coaxial extrusion printing technique, a novel 3D printing method, provides a simple approach to engineer microchannel structures via a coaxial nozzle to control the deposition of biomaterials [4]. It is demonstrated that coaxial printing can fabricate vessel-like tubes directly with tunable diameters from micron to millimetre and large-scale lengths [5,6]. Gao et al. fabricated vessel-like alginate-based microtubes through coaxial printing and these obtained vascular tubes with multilevel channels commendably mimic the microenvironment of vessels [7]. Meanwhile, Hong et al. have reported a coaxial bioprinting method for direct fabrication of cell-laden tubular structures and the cells were distributed along the tube axis [8]. These previous studies on vessel-like tubes through this coaxial extrusion printing method mainly

* Corresponding author. Shenzhen Institutes of Advanced Technology, Chinese Academy of Sciences, Shenzhen, 518055, PR China
E-mail address: cs.ruan@siat.ac.cn (C. Ruan).

https://doi.org/10.1016/j.bioactmat.2020.10.028
Received 4 August 2020; Received in revised form 26 October 2020; Accepted 28 October 2020

focused on the improvement of the printability of biomaterial-based inks to obtain the shape-similar hollow tubes. However, whether or not these printed vessel-like tubes can realize the functional features of small-diameter artificial vessels still remains unknown [9].

For small-diameter artificial vessels, endothelialization during the initial stage is an effective avenue to prevent the occurrence of thrombosis formation and intimal hyperplasia after transplantation [10,11]. As is known to all, endothelialization is a relative slow process, which is unable to immediately function at the initial stage of implantation [12,13]. Thus, it is a common strategy that introduction of appropriate anticoagulants into artificial vessels for rapid antithrombogenicity before startup of endothelialization [14,15]. Previous investigations have demonstrated that surface modification, including the biophysical cues (smooth, hydrophilicity, porosity and lamellar nano-topography) [16–18] and biochemistry cues (growth factors, cytokine, nitric oxide, functional drugs and so on) [19–22], could be applied for promoting the anticoagulation and endothelialization of small-diameter artificial vessels for blood grafts. However, achieving a small-diameter artificial vessel with a biologically inspired release system that sequentially release in spatiotemporal coordination of dual molecules for rapid antithrombogenicity and endothelialization via a surface modification method remains a great challenge.

Motivated to address the above challenges, we aim to develop a small-diameter vessel-like tube with a biologically inspired release system to mimic the sequential requirements for antithrombogenicity and endothelialization for potential application of artificial vessels via a coaxial printing technique and electrostatic layer-by-layer (LbL) technology (Fig. 1). In particular, a polyelectrolyte-based material comprising of sodium alginate (SA) with negative charges and ε-polylysine (ε-PL) with positive charges is used as the ink for coaxial printing of vessel-like tube. According to our previous study, this polyelectrolyte SA/ε-PL ink with an excellent self-supporting property facilitated the fabrication of tube structure and then the surface charges of their corresponding 3D-printed scaffolds could be easily regulated to facile biofunctionalization [23]. Then, two bioactive molecules, heparin and pentapeptide Tyr-Ile-Gly-Ser-Arg (YIGSR), are further deposited on the polyelectrolyte-based tube surface to engineer functional coatings via the electrostatic LbL technology. Heparin is a common negatively charged drug for anticoagulant clinically. Surface functionalized with heparin has been reported as superior way to protect blood contacting biomaterials from thrombus formation [24,25]. YIGSR is a functional motif of laminin that binds to the laminin receptor, of which the isoelectric point (pI) is about 8.75. YIGSR is confirmed to enhance endothelialization via improvements on migration speed and preferred directional migration behaviors of endothelial cells (ECs) [26,27]. It is expected that the sequential release of heparin and YIGSR resulting from the electrostatic interaction can construct a biologically inspired release system, beneficial for the antithrombogenicity and endothelialization in a logical manner.

2. Materials and methods

2.1. Materials

Sodium alginate (SA) (low viscosity) and toluiding blue were purchased from Sigma-Aldrich (St Lousis, USA), ε-polylysine (95%, ε-PL) was brought from Macklin company (Shanghai, China), 1-ethyl-3-(3-dimethylaminopropyl) carbodiimide (98%, EDC), N-hydroxysuccinimide (98%, NHS), 2-(N-morpholino) ethanesulfonic acid monohydrate (99.5%, MES) were purchased from Aladdin (Shanghai, China), Tyr-Ile-Gly-Ser-Arg (YIGSR) was brought from Bankpeptide Inc (Hefei, China), heparin was brought from Shanghai Yuanye Bio-Technology (Shanghai, China), micro BCA protein assay kit was purchased from Shangon Biotech (Shanghai, China), human umbilical vein endothelial cells (HUVECs) and the culture medium for HUVECs were brought from Cyagen Biosciences (CA, USA), human pulmonary artery smooth muscle cells (HPVSMCs) and the culture medium for HPVSMCs were brought from ScienCell (CA, USA). All the other reagents were used as received without further purification.

2.2. Coaxial printing of hollow tube

The polyelectrolyte-based hollow tubes were fabricated by coaxial printing method using a multi-channel bio-plotter pneumatic dispensing

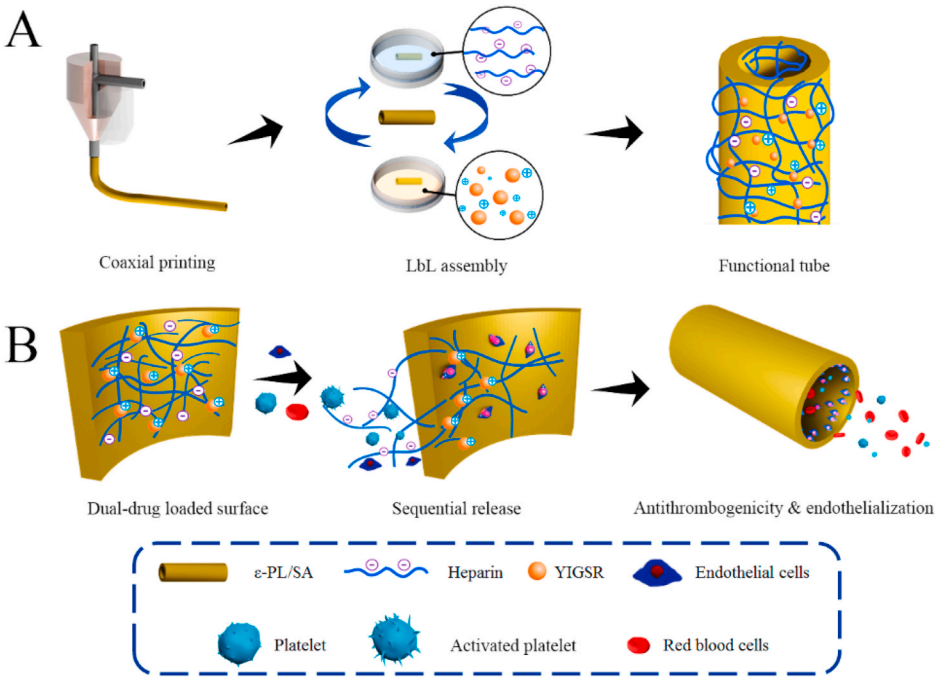

Fig. 1. Schematic illustration of (A) coaxial-printed ε-PL/SA tubes modified with heparin and YIGSR via electrostatic LbL assembly, and (B) a smart release system that dual drugs were sequential released spatiotemporal coordinately so that to promote antithrombogenicity and endothelialization.

system (Bioscaffolder 3.1, GeSiM, Germany). ε-PL and SA were dissolved in distilled water and mixed homogeneously with continually sharply stirring. Then the obtained viscous polyelectrolyte-based composites were used as the printing ink and loaded into a printing tube that connected with a designed coaxial nozzle. Then the hollow tubes were directly fabricated by extruding printing ink in a proper speed at a printing stress of about 550 kPa at room temperature. To ensure the printability, the concentration of SA in distilled water was fixed to 40%, and the ratios of ε-PL to SA of the printing ink were 0.25, 0.5, 1 and 2 that were based on the molecular ratio of amino groups of ε-PL and carboxyl groups of SA. And the diameter of tubes fabricated by serials of coaxial nozzles were measured to study the shape fidelity. The hollow tubes were dipped into 0.5 M EDC/NHS (EDC: NHS = 2: 1) in MES solution with pH = 6.5 for 1 h to solidify. Meanwhile, film samples of polyelectrolyte-based composites were prepared by solvent casting technology for further test.

2.3. Swelling and degradation

The swelling properties of film samples were evaluated by a weighing method, and the variation in diameters of the hollow tubes incubated in different pH solutions were further evaluated using a digital micrometer. The initial mass of the dried film samples (n = 3) was recorded and marked as Wd, and then samples were immersed in the PBS solution at 37 °C. After 24 h, samples were weighed again after the liquid on the surface of films was wiped off, and the mass without obviously changes was recorded and marked as Ws until the swelling equilibrium was reached. To ensure the swelling equilibrium was reached, the dynamic swelling behaviors was also monitored. The swelling ratio (Q) was determined as follows:

$$Q = \frac{Ws \times 100\%}{Wd} \quad (1)$$

The degradation assessment (n = 3) was performed in the same way with prolonged incubation time, of which the onset time was taken at the point when the sample was reached the swelling equilibrium, thus it was recorded and marked as Ws. The degraded samples were taken out and weighed at special time intervals, the obtained data were set as Wt. The weight loss ratio was calculated as follows:

$$\text{Weight loss ratio} = \frac{(Ws - Wt)}{Ws} \times 100\% \quad (2)$$

2.4. LbL assembly coating construction

For the construction of functionalized surface of hollow tubes, the biological inspired smart release coating was fabricated onto the substrate surface of hollow tubes via electrostatic LbL self-assembly. Briefly, self-assembly proceeded by immersing the substrate alternatively into 1.0 mg/ml of heparin solution (pH = 4.5, polyanion) and 0.5 mg/ml YIGSR solution (pH = 4.5, polycation) for 10 min. After each immersion step, the sample was rinsed by distilled water for 3 times. The final films or vascular-like tubes containing different number of heparin/YIGSR bilayers were denoted as ε-PL/SA-X-Y, where X was the ratio of ε-PL to SA, and Y was the number of heparin/YIGSR bilayers. For example, ε-PL/SA-0.25-5 represented the sample with the ε–PL/SA ratio of 0.25 and the heparin/YIGSR bilayers number of 5.

2.5. Material characterization

Morphological observation of the prepared samples was performed by a field emission scanning electron microscope (SEM, ZEISS SUPRA 55, Zeiss, Germany) that equipped with an Energy Dispersive Spectrometer (EDS), and the macroscopy of the hollow tubes were also observed by a 3D microscope (RH-2000, Hirox, Japan). Before SEM observation, all samples were lyophilized and then coated with platinum for 30 s. To characterize the variances of material functional groups, Fourier transform infrared spectroscopy (FTIR) with potassium bromide pellet was used and tested in the wavenumber range of 600–4000 cm^{-1} before and after the LbL assembly. Mechanical properties of the hollow tubes were evaluated by a tensile test, which performed in an electronic universal materials test machine (IBTC-300SL, CARE, China). Five samples from each group were measured and all samples were soaked in phosphate-buffered saline (PBS) solution (pH = 7.4) for 30 min at room temperature before testing. The rectangular specimen ends were vertically mounted on the machine with a 30-N load cell with a 10-mm distance for mechanical loading. The loading speed was 6 mm/min and the testing data were recorded and used for calculating stress-strain curves. The maximum tensile strength, elastic modulus, and elongation at break were calculated from stress-strain curves in accordance with the accepted formulas.

2.6. Contact angle measurement and particle size test

The pendant water drops contact angle of ε-PL/SA film coated with heparin and YIGSR was performed on an optical contact angle meter (Theta Lite, Biolin, Sweden). Sample films were first stuck flat on a glass slide, and using a syringe, at least 5 μL of double distilled droplet were placed in the film surface, then images were recorded using a color CCD camera. The contact angle between the film surface and the double distilled droplet was measured using a goniometer. The average contact angle value and the standard deviation in the contact angle were calculated (n = 3).

Transmission electron microscope (TEM, JEM-3200 FS, JEOL, Japan) Malvern Panalytical Nano-particle Analyzer (Zetasizer Nano ZS, Malvern, England) were used to observe the aggregate morphology and particle size of heparin and YIGSR complex in different pH. Heparin and YIGSR were dissolved in the sodium acetate buffer solution with pH = 5.0, PBS solution with pH = 7.4 and Tris-HCl solution with pH = 8.0, respectively. The concentration of heparin was 0.1 mg/ml and of YIGSR was 0.05 mg/ml. Furthermore, heparin was dissolved in the PBS solution with pH = 7.4 and the concentration of heparin was 0.1 mg/ml. Then the prepared sample solutions were dropped onto the copper mesh with ultra-thin carbon film, and samples were dried at room temperature for TEM, and the prepared solutions were also measured by Zetasizer Nano ZS to study the diameter of heparin and YIGSR complex particles.

2.7. Immobilization and controllable release of heparin and YIGSR

The classical toluidine blue method was used to determine the amount of immobilized heparin. Toluidine blue solution was prepared by mixing the toluidine blue reagent (0.005 w/v %) and NaCl (0.2 w/v %) in HCl (0.01 M) solution. Then the toluidine blue solution was reacted with a series of standard heparin of known concentration to form heparin/toluidine complex, which was extracted and removed by the addition of hexane. The absorbance of the leaving unreacted heparin aqueous solutions was measured at 630 nm. The standard curve was established with standard heparin solution so that the absolute amount of heparin immobilized on samples could be calculated. Similarity, to calculate the amount of immobilized YIGSR on samples, the standard curve of YIGSR with known concentration was obtained using micro BCA protein assay kit according to product instruction.

Release behaviors of LbL assembly coating consisted of heparin and YIGSR were performed in static environment at 37 °C. The coated film samples (8 mm × 8 mm) were incubated in 2 ml of PBS (pH = 7.4) solution or other solutions (pH = 5.0 and 8.0), and the solution was collected at pre-determined time intervals and same volume of solution was added. The dual-drug releasing solution was divided into two at 9: 1 of volume for the quantification of heparin and YIGSR released from the coating, respectively. The amounts of drugs immobilized were quantified by directly calculating all the releasing quantification monitored

using UV–Vis spectrophotometry.

2.8. Hemolysis and platelet adhesion

The hemolysis test and platelet adhesion test of the vascular graft were conducted according to ISO 10993-4-2017. Animals care and treatment were performed in accordance with the Institutional Animal Care and Use Committees (IACUC) guidelines of Shenzhen Institutes of Advanced Technology, CAS. Fresh blood was obtained from an adult male New Zealand white rabbit (1.0-year-old) and stored in the blood collection tubes with citrate anticoagulant at 4 °C. For the hemolysis test, diluted blood was prepared from the fresh anticoagulant blood that was diluted in normal saline with the volume ratio of 4:5, and the absorbance of 0.2 mL diluted blood in 10 mL normal saline was adjusted to 0.8 ± 0.3 at 545 nm. The graft samples rinsed with normal saline were placed in 24-well culture plate, and incubated in 10 mL normal saline at 37 °C for 30 min. Then 0.2 mL diluted blood was added into the tube and incubated for another 60 min. Furthermore, 10 mL normal saline and distilled water mixed with 0.2 mL diluted blood were served as negative control and positive control, respectively. Subsequently, the solutions were transferred and centrifuged at 1200 rpm for 5 min. The collected supernatant was measured by a spectrophotometer at 545 nm. Three specimens were tested for each sample. Hemolysis rate was calculated:

$$\text{Hemolysis rate } (\%) = \frac{\text{As} - \text{An}}{\text{Ap} - \text{An}} \times 100\% \quad (3)$$

Where As, An and Ap was represent the absorbance of the experimental sample, negative control and positive control, respectively.

For the platelet adhesion test, platelet-rich plasma (PRP) was extracted from the whole rabbit blood by centrifuging at 1500 rpm for 15 min samples were first incubated in PBS at 37 °C for 30 min. Then PBS was removed gently and 500 μL PRP was added to the sample surfaces. Samples were incubated at 37 °C for 2 h, which were dipped into PBS and shaken carefully to remove loosely adhered platelets. After fixing with 2.5 wt % glutaraldehyde in PBS at 4 °C for 24 h, samples were dehydrated by a series of ethanol solution washes (50%, 70%, 80%, 90%, and 100%) and dried in a 37 °C oven. Three replicates were used for this test. To study the antithrombotic behavior, the adherent platelets on the graft surface were observed by SEM. Statistical analysis was performed based on five images randomly selected from different fields for each sample. In addition, the collected whole rabbit blood was dilute in diluted in normal saline with the volume ratio of 5:5 and it was used to study the deposition of composites of blood on the prepared sample surface according to the platelet adhesion test.

2.9. In vitro cytocompatibility

CCK-8 assay was used to evaluate HUVECs and HPVSMCs proliferation cultured on the film samples of ε-PL/SA. HUVECs and HPVSMCs were obtained and cultured with the matching culture medium which prepared according to the manufacture' instruction. Samples were placed in the 24-well culture plate, and rinsed with sterile PBS for three times. The cultured cells then were seeded at a density of 1.0×10^4 cells per well and cultured for 1, 3, 5 days. The culture medium was refreshed every two days. The viability of HUVECs and HPVSMCs seeded on the samples was quantified at the predetermined intervals by CCK-8 assays which measured the absorbance at 450 nm using a microplate reader (Multiskan GO, Thermo Scientific).

Live/Dead viability kit was performed to study the behaviors of HUVECs seeded on the samples. Briefly, HUVECs were embedded into a 24-well culture plate placed with vascular graft samples, and cell viability was assessed after 1 day and 5 days culturing period followed the staining protocol according to the product instruction. The green fluorescent calcein-AM and the red fluorescence ethidium homodimer-1 (EthD-1) was used to indicate the living cells and death cell, respectively. Stained Samples were observed and imaged by fluorescent microscope system (BX53, Olympus, Japan). And then the samples were rinsed with PBS solution carefully, fixed with 2.5 wt % glutaraldehyde and dehydrated by a series of ethanol solution washes for SEM observation.

2.10. Statistical analysis

Experimental data were represented as mean ± standard deviation. Statistical analysis was carried out by one-way ANOVA using a Bonferroni analysis. Statistical significance was represented as * $p < 0.05$, and ns, means no significant difference.

3. Results and discussion

3.1. Coaxial printed biomimetic hollow tubes for vascular graft

In this study, a series of coaxial printed ε-PL/SA hollow tubes for vascular graft have successfully prepared through a customized coaxial nozzle. We have designed and prepared coaxial nozzles with different diameter (Fig. S1, Supporting Information), and ε-PL/SA polyelectrolyte mixture solution was prepared for printing the tube. It was believed that how to maintain the hollow structure, especially, without the cross-linked agent or supporting materials during the printing process is one of the biggest problems of coaxial extrusion to fabricate tubes. Compared to the SA scaffold that cross-linked with Ca^{2+}, the printed ε-PL/SA tubes were more stable to maintain the hollow structure before and after chemically cross-linked with EDC/NHS solution due to the electrostatic interactions [23]. We finally determined that the ink component ratios of ε-PL to SA were 0.25, 0.5, 1 and 2, then the hollow tubes with different sizes were printed with the customized nozzles, as shown in Fig. 2A and B and Fig. S2 (Supporting Information), the engineered tubes were demonstrated with high fidelity, smooth surface and stable structure. The structure of the printed tubes was improved by tune the concentration of inks and the printing parameters, and the shape of the tubes were displaying round or nearly round, the wall thick of the tubes was uniform, though the perfused tubes were obtained directly without cross-linked agent or supporting materials. Meanwhile, the inner diameter of the printed tubes could be regulated from about 1300 to 630 μm, and wall thicknesses could be also tuned by altering the diameter of coaxial needle (Fig. 2C). SA inks with excellent printability had been used to prepare hollow tubes by using coaxial extrusion, but these reported tubes were demonstrated with only small diameter, which should be prone to collapse and blockage [4,28]. In order to increase the diameter of printed tubes and enhance the stability of hollow structure during the coaxial extrusion process, in this study, ε-PL was added and effectively improved the stability of the printed scaffold via charge-charge interaction (electrostatic interaction). Additionally, the ε-PL/SA polyelectrolyte tubes with the diameters that were larger than 1300 μm or smaller than 630 μm could be also fabricated by further optimizing the contents of ε-PL/SA or the diameter of coaxial nozzle.

The morphology, swelling behavior, mechanical properties and degradation of ε-PL/SA based tubes were further explored. The morphology of tubes was observed by using SEM and 3D microscopy. It was found that the irregular micropores on the ε-PL/SA-0.5 surface was much more than the others (Fig. 2D), and showed a fully interconnected microvascular network within the micro-structured tube matrix structure which benefit for transporting nutrition (Fig. S3, Supporting Information). It was indicated that the cross-linked density was increased with the addition of ε-PL, however the abundance of ε-PL chain segments would fill the pore structure, resulting in a reduction of pores of ε-PL/SA-2. The swelling behavior of ε-PL/SA-0.25, ε-PL/SA-0.5, ε-PL/SA-1 and ε-PL/SA-2 was assessed (Fig. 2E, **F**), and the dynamic swelling behavior of them were measured to ensure reach the swelling equilibrium (Fig. S4, Supporting Information). The swelling ratio was increased and then decreased with the ratio of ε-PL to SA increased, and the

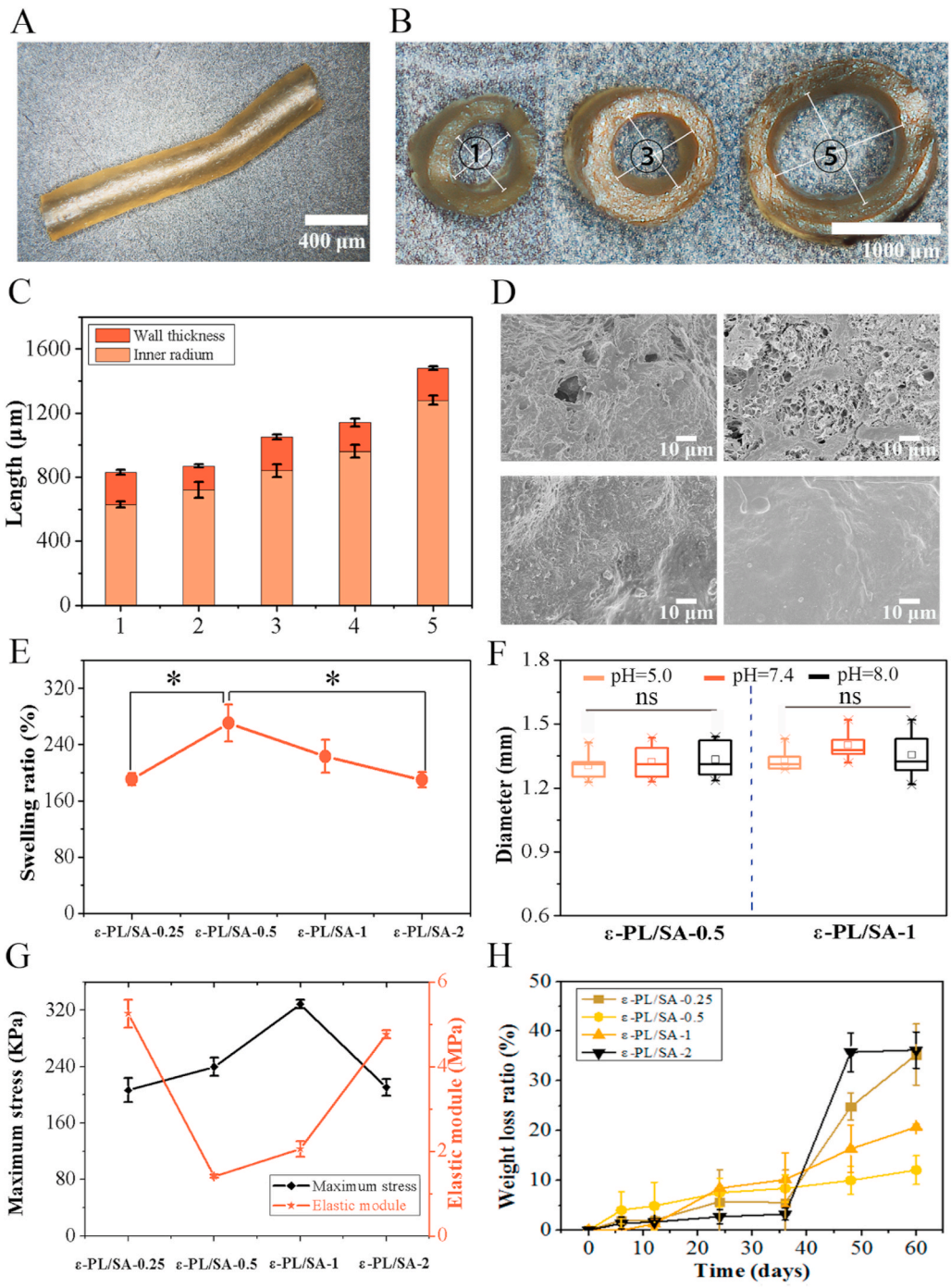

Fig. 2. (A) The representative image of ε-PL/SA hollow tube observed by 3D microscope. (B) Macrophotography of three hollow tubes with different sizes printed with the customized nozzles. (C) Analysis of the wall thickness and inner diameter of ε-PL/SA hollow tubes. (D) Microscopic appearance of ε-PL/SA hollow tubes observed by SEM. (E) The swelling behavior of ε-PL/SA hollow tube. (F) Diameter measurement of ε-PL/SA-0.5 and ε-PL/SA-1 incubated in pH = 5.0, 7.4 and 8.0. (G) Maximum stress and elastic module of ε-PL/SA based hydrogels. (H) 3D printed tubes weight loss over two months of immersion in PBS solution.

swelling ratio of ε-PL/SA-0.5 was the largest (270.4 ± 26.4%). Notably, the diameters of ε-PL/SA-0.5 tube and ε-PL/SA-1 tube incubated in pH = 5.0, pH = 7.4 and pH = 8.0 were not significant changed, which means that the diameter of the printed ε-PL/SA tubes would be unchangeable or less changing under the dynamic microenvironment. It also improved the mechanical properties of the tube (Fig. 2G, and Fig. S5, Supporting Information). The maximum stress and elastic module were increased and then decreased with the ratio of ε-PL to SA increased. Therefore, the internal structural properties of the tube affect the swelling and mechanical properties of the printed tubes. The results have proved that the tube was becoming flexible and strong instead of brittle and weak. Unlike Ca^{2+}/Alginate hydrogel that unstable in PBS solution reported by some previous literatures [6,29], the degradation rate of the tubes was obviously slow down after the treatment of EDC/NHS, as shown in Figure Fig. 2H, and the weight loss ratio of ε-PL/SA-2 was about 3% after incubating in PBS solution for 36 days at 37 °C. In addition, during the degradation process, the composites of ε-PL/SA based tubes were firstly dissolved into the PBS solution, and finally the tubes were cracked into pieces. These results showed that the stability, priority and mechanical properties of ε-PL/SA composites were excellent to print hollow tubes for vascular graft.

3.2. *Functional coatings fabrication and characterization*

Natural ECM has the characteristics of polyelectrolyte, which can realize the immobilization, storing and release of multiple signal

molecules through electrostatic interaction, and regulate the signal molecules in time and space [30]. In this study, the dual drugs with opposite charges, heparin and YIGSR, were designed to form a functional coating by electrostatic LbL self-assembly on the inner surface of the ε-PL/SA polyelectrolyte-based hollow tubes. Among them, heparin is a medium strong acid, which is negatively charged in aqueous solution as the dissociation of Na^+, while YIGSR is positively charged under pH < pI (8.75). Both of heparin and YIGSR were deposited on the hollow tube surface layer by layer via electrostatic interaction. In order to identify the existence of heparin and YIGSR on the polyelectrolyte-based composite surface, SEM, FTIR and EDS were carried out, and the quantity of heparin and YIGSR was evaluated by Ultraviolet–visible spectroscopy. As shown in Fig. 3A, compared with the ε-PL/SA films without any depositions, the surface with a functional coating was changed from smooth to rough, and heparin/YIGSR complex filaments were obviously observed on the surface of ε-PL/SA based films. It was showed that the number and form of the heparin/YIGSR complex filaments was different as the charge was tunable by the ratio of ε-PL to SA. The more deposition layers were, the more content of heparin and YIGSR were. FTIR spectra (Fig. S6, Supporting Information) and EDS (Fig. 3B) were further demonstrated the heparin/YIGSR complex was deposited on the surface of ε-PL/SA films. Compared to the FTIR spectra of heparin, YIGSR, ε-PL/SA, the coated ε-PL/SA with heparin and YIGSR showed peaks at 3718 cm^{-1}, 2870 cm^{-1}, 1412 cm^{-1} and 705 cm^{-1}, which should be attributed to the introduction of heparin and YIGSR, the peak at 3718 cm^{-1} could be attributed to the introduction of heparin which shift form 3614 cm^{-1} and the peak at 1412 cm^{-1} was also assigned to the introduction of heparin. Furthermore, the peaks at 1412 cm^{-1} and 705 cm^{-1} were assigned to the introduction of YIGSR. Through the elemental mapping examination, C, N, O, S and Na elements were found to uniformly distribute on the ε-PL/SA based vascular graft surface, which were further verified by the EDS spectrum (Fig. 3B). It was demonstrated the successful deposition of heparin and YIGSR on the substrate surface, especially the distribution of S element proved the existence of heparin.

The coating should be a profound influence on the biomaterials surface such as the hydrophilicity that measured by using the water contact angle experiment (Fig. 3C). The results showed that as the number of dual-drug deposition layers increased, the contact angle increased from 45° to 63°, thus the hydrophilicity of the tube surface decreased significantly. The decreased hydrophilicity of the tube with coating was facilitated the cell adhesion due to the high hydrophilicity of biomaterials would impede the attachment of cells, and the YIGSR was facilitated as well. In order to measure the content of heparin and YIGSR on the surface of the printed tubes and analysis of the drug release behavior later, we have established the standard curve for heparin and YIGSR, respectively (Fig. S7, Supporting Information). Thus, the drug content immobilized on the surface of the tubes were determined (Fig. 3D and E). It showed that the content of heparin and YIGSR were increased with the number of assembly layers increased, and the deposited heparin on the tube was more than YIGSR. It indicated that though heparin and YIGSR were deposited on the surface via electrostatic interaction, there are chains entanglement in thin coatings to form a stable physical cross-linked network filled with YIGSR that was also act as a cross-linked point between the heparins and tube surface. Additionally, the deposition quantity of heparin and YIGSR on ε-PL/SA-0.5-9 were the most. It also supported that adsorption of heparin and YIGSR on the ε-PL/SA tubes was not only influence by the residual amine groups after the treatment of EDC/NHS, but also influence by the rejection between heparins and ε-PL/SA tube substrate. Furthermore, the nine dual-layer assembly were chosen to optimize the contribution of bioactive components and improve the immobilization of heparin and YIGSR.

3.3. Sequential release behavior characterization

It was believed that the interactions between biomaterials and cells are mainly relied on the physicochemical properties of the ECM surface microenvironment [31]. The drug coating could improve the surface characteristics and provide functional domain for the vascular graft to promote the tissue restore and regeneration. In this study, heparin and YIGSR were successfully immobilized on the surface of the negatively charged matrix through electrostatic interaction. Heparin/YIGSR coating was aimed to form a sequential release system that heparin would release at first and sustained to prevent the thrombogenicity, and then the YIGSR would release to recruit endothelial cells for promoting the endothelialization. The release behaviors of heparin and YIGSR on the ε-PL/SA-0.25-9, ε-PL/SA-0.5-9, ε-PL/SA-1-9 and ε-PL/SA-2-9 were

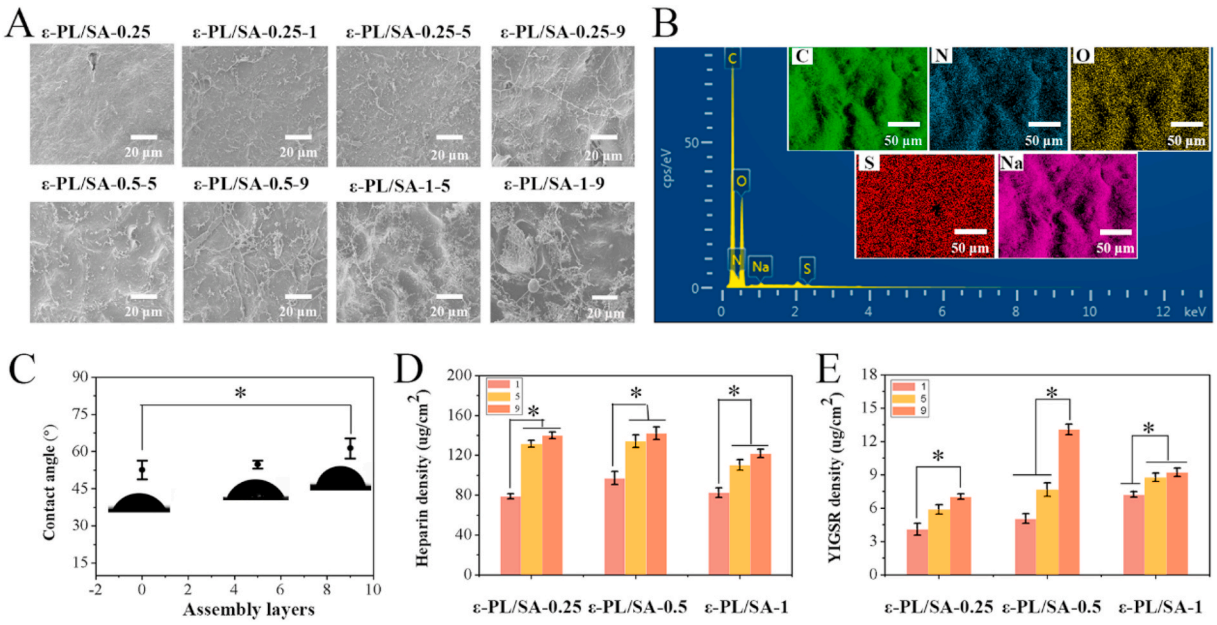

Fig. 3. (A) SEM micrographs of different ε-PL/SA tube coated with or without heparin and YIGSR. (B) EDS spectrum of C, N, O, S and Na elements on the surface of dual-drug coated ε-PL/SA. (C) Contact angle values recorded for the prepared ε-PL/SA films coated with heparin/YIGSR. (D) Adsorption of heparin at a concentration of 1 mg/ml after LbL Assembly. (E) Adsorption of YIGSR at a concentration of 0.5 mg/ml after LbL assembly.

studied under physiological environment pH = 7.4 (Fig. 4A, B, C and D), and it was indicated that the ε-PL/SA based tubes reveal negatively charged in pH = 7.4 solutions. Generally, it showed that the drugs release behaviors of these four samples showed a surprisingly same trend which meet the design goal, but it was not presented in the solution of pH = 5.0 and pH = 8.0 (Fig. S8, Supporting Information). We have divided the release process into two stages. In the first stage, the two bioactive molecules were burst release initially which usually happen on the non-covalent bond release system, and then they were continued to release at a slower speed. Furthermore, the release speed of YIGSR was much slower than of heparin. The amount of heparin released from coating would be resisted the acute postoperative thrombosis. In the second stage, the release speed of YIGSR was much faster than of heparin, and much YIGSR was released from the coating due to the physical network was damaged while the heparin was less released. Therefore, the release behavior has showed a potential sequential release characteristic for multiple signal molecules releasing and functional integration.

The hypothesis was provided to explain the release behavior of heparin/YIGSR coating according to the long-range electrostatic interaction [32] and the theory of electric double layer. The hypothesis indicated that negative charged heparin and positive charged YIGSR were assembled to from heparin/YIGSR complex which deposited layer by layer on the negative charged biomaterial's surface, and the molecular chain entangled to form physical network through electrostatic interaction. The stability of heparin/YIGSR complex was influenced by the quantity of negative charge on the ε-PL/SA substrate surface and the pH of solution. YIGSR was stored in the physical network and act as the cross-linked point between negatively charged molecular chains. When heparin/YIGSR complex was dissociated, heparin was released to the local, and YIGSR would draw back into the network, due to the electrostatic attraction force to YIGSR and the electrostatic repulsion force to heparin. Therefore, the electrostatic interaction between ε-PL/SA and heparin/YIGSR complex regulated the sequential release of heparin and YIGSR, as shown in Fig. 4E. In addition, the quantity of negative charge was changing with the pH of the solution changed, due to the ionization of SA that is a strong base and weak acid salt, and the positive changed YIGSR peptide was weakened when the pH of the solution increased.

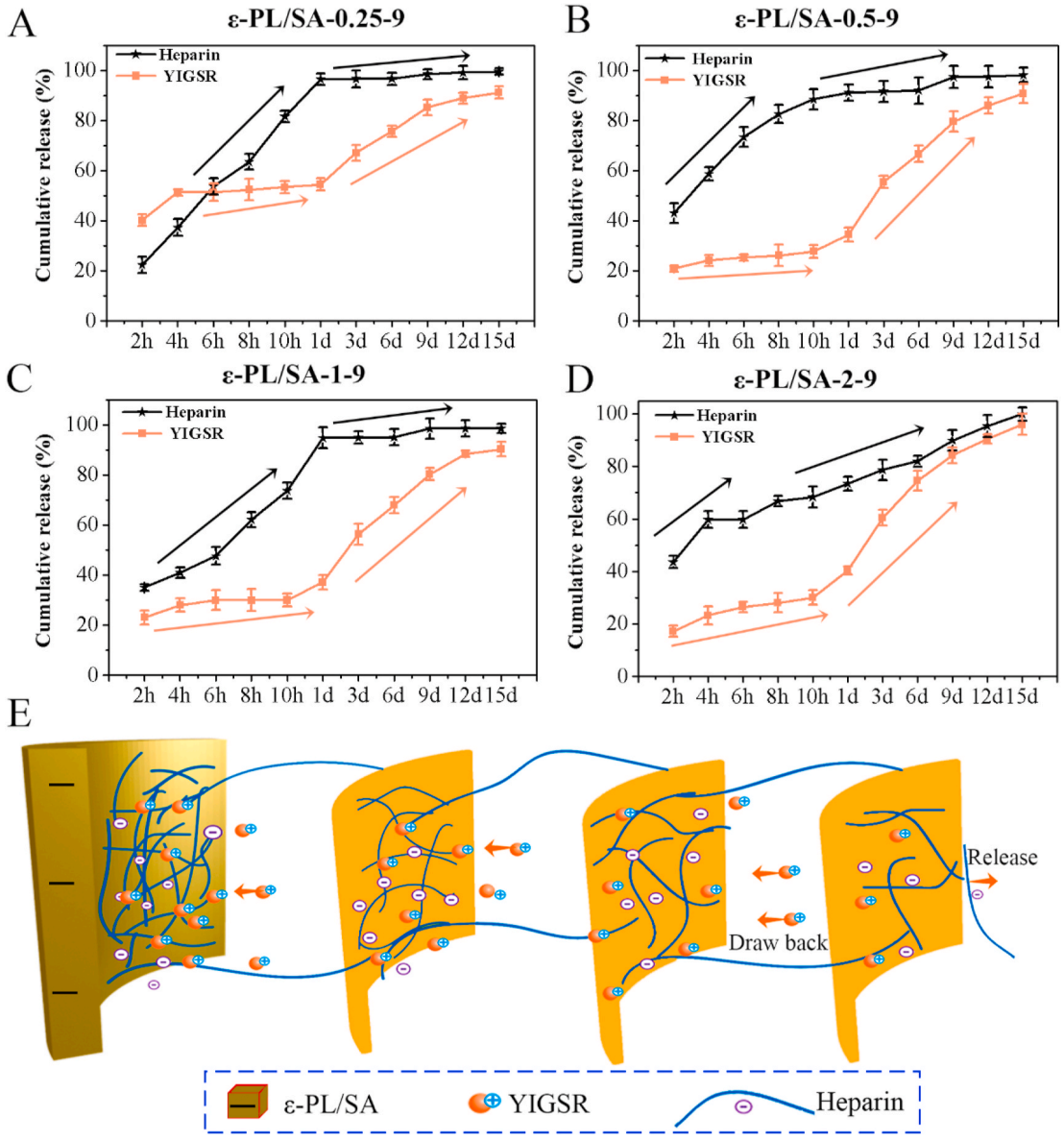

Fig. 4. The release behaviors of heparin/YIGSR coatings on the (A) ε-PL/SA-0.25-9, (B) ε-PL/SA-0.5-9, (C) ε-PL/SA-1-9 and (D) ε-PL/SA-2-9 were studied in pH = 7.4 solution. (E) Schematic illustration of the sequential release of heparin and YIGSR.

The TEM and Zetasizer Nano ZS were performed to study the diameter of heparin in the solution of pH = 7.4, heparin/YIGSR complex in the solutions of pH = 5.0, 7.4, and 8.0, respectively. It was proved that the heparin/YIGSR complex particles in the solutions of pH = 5.0 and 8.0 were tightly combined into small nanoparticles due to the electrostatic interactions, and the particles diameter was much less than the heparin/YIGSR complex in the PBS solution of pH = 7.4 (Fig. S9 and Fig. S10, Support Information). As seen from Fig. S10 (Support Information), the heparin particles diameter in the PBS solution of pH = 7.4 was reached about 4507 nm while the heparin/YIGSR complex particles was about 487.2 nm, 352.2 nm and 232.2 nm in the solution of pH = 7.4, 5.0 and 8.0, respectively. Furthermore, compared with the particle size measured by TEM, the particle size measured by Zetasizer Nano ZS was much larger due to the observation of hydrodynamic size that corresponded to the core and the swollen corona of the micelles. For example, the heparin/YIGSR complex particles diameter in pH = 7.4

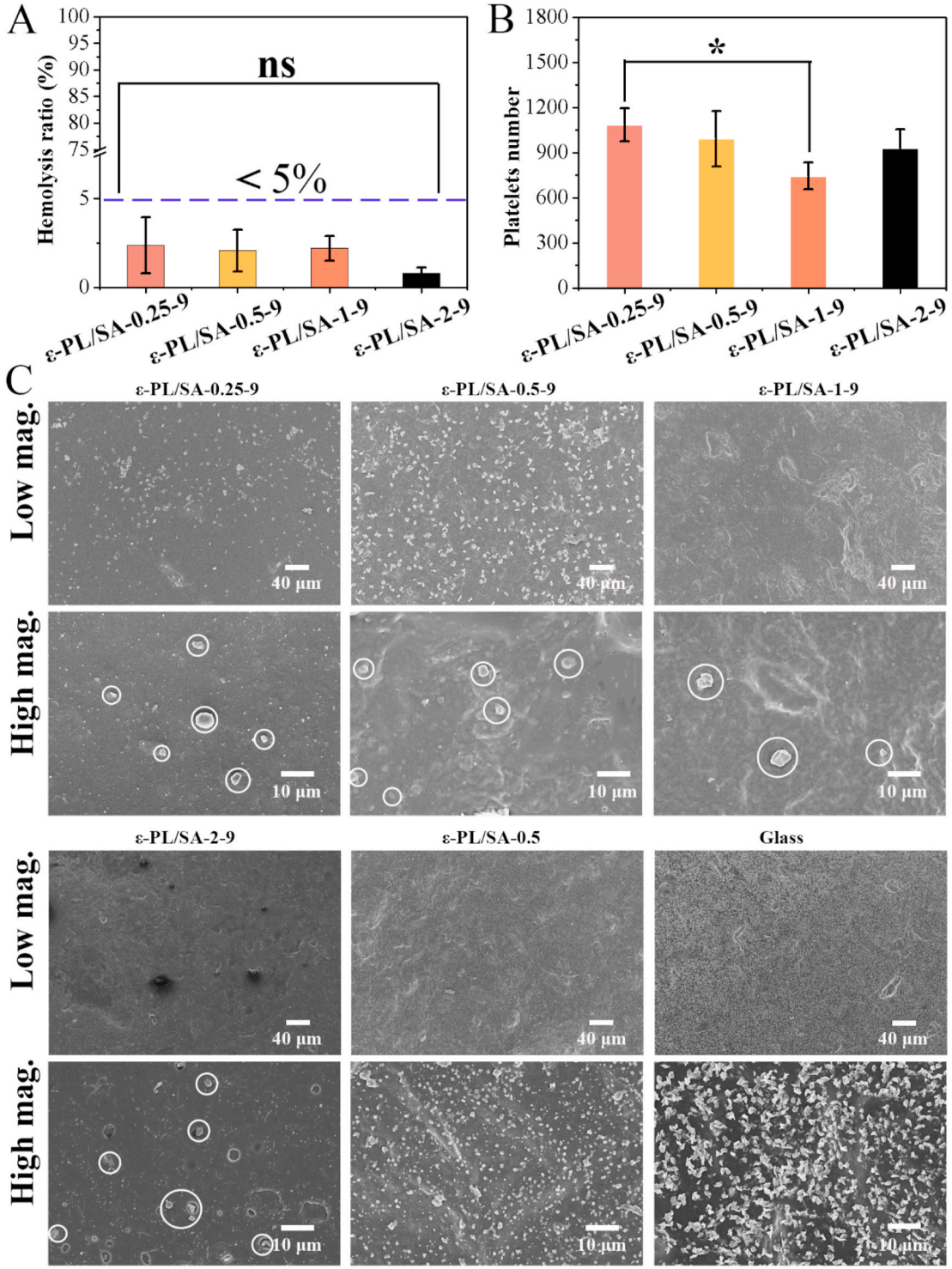

Fig. 5. The hemocompatibility testing. (A) Hemolysis rate for ε-PL/SA-0.25-9, ε-PL/SA-0.5-9, ε-PL/SA-1-9 and ε-PL/SA-2-9. (B) Statistical results of the number of platelets attached. (C) Representative SEM images of ε-PL/SA-0.25-9, ε-PL/SA-0.5-9, ε-PL/SA-1-9, ε-PL/SA-2-9, ε-PL/SA-0.5 and glass at low and high magnifications. The platelets attached on ε-PL/SA-0.25-9, ε-PL/SA-0.5-9, ε-PL/SA-1-9, ε-PL/SA-2-9 were marked with white circle.

solution was about 270 nm observed by TEM, however it was about 487.2 nm measured by Zetasizer Nano ZS. When the coated graft incubated in the solution of pH = 5.0 or pH = 8.0, the sequential behavior of the coating was not obviously observed in Fig. S8 (Support Information), it is because that heparin/YIGSR complex was difficult to be dissociated and then sequential release.

3.4. Hemocompatibility of the ε-PL/SA based tubes with functional coatings

Small diameter vascular grafts have low patency and failed in animal experiments due to the poor hemocompatibility, especially acute postoperative thrombosis. In this study, the blood compatibility of the ε-PL/SA based tubes was evaluated by the hemolysis test and platelet adhesion experiments (Fig. 5 and Fig. S11, Supporting Information). Fig. 5A

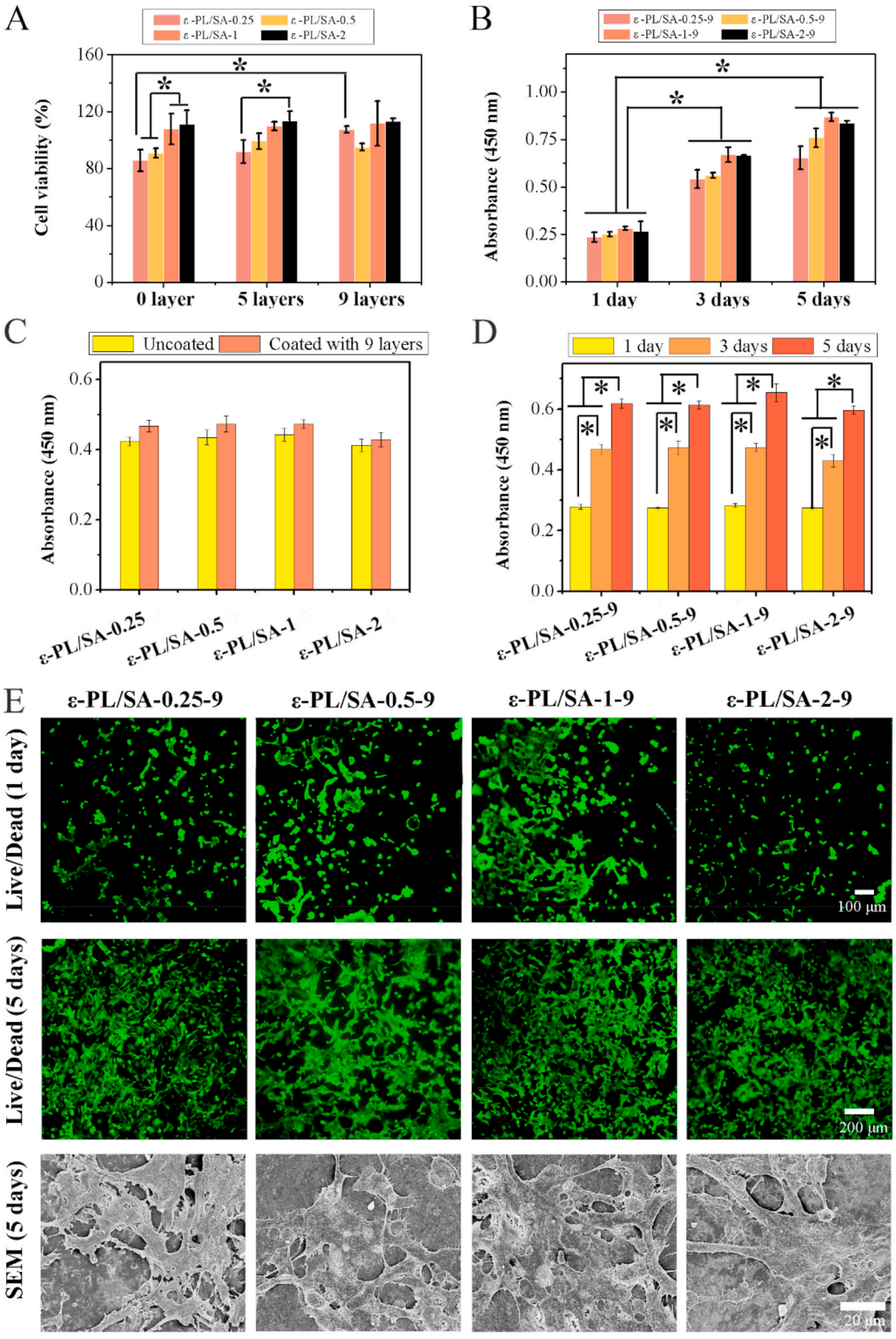

Fig. 6. CCK-8 assay was used for evaluating the cell viability of HUVECs cultured on (A) samples with different coating layers for 3 days and (B) ε-PL/SA-0.25-9, ε-PL/SA-0.5-9, ε-PL/SA-1-9 and ε-PL/SA-2-9 for 1, 3, 5 days. CCK-8 assay was used for evaluating the cell viability of HPVSMCs cultured on (C) samples coated without or with 9 heparin/YIGSR layers for 3 days and (D) ε-PL/SA-0.25-9, ε-PL/SA-0.5-9, ε-PL/SA-1-9 and ε-PL/SA-2-9 for 1, 3, 5 days. (E) The spreading and proliferation of HUVECs cultured for 1 day (upper row) and 5 days (middle row) were directly stained by LIVE/DEAD viability kit, and HUVECs cultured for 5 days was also investigated by SEM (bottom row).

showed the results of the hemolysis test in vitro that the hemolysis rate of the four groups was less than 5%, indicating that ε-PL/ SA composite is not hemolytic activity to red blood cells, and there is no significant difference in all groups. As we all known, hemolysis is the disruption of red blood cells, which causes the release of hemoglobin. The prepared composite films incubated with the whole blood did not cause the lysis of red blood cells, should be due to that the sample was stable due to the characteristics of polyelectrolyte (such as maintaining the pH of solution), and the components were natural products and biocompatible. Fig. 5B and C were the results of platelet adhesion on the coated ε-PL/SA based films, and the uncoated ε-PL/SA-0.5 film and glass were used as the control group. Fig. 5B was the statistical analysis results based on the SEM image of the platelet adhesion. The number of platelets attached to ε-PL/SA-1-9 films were the least in all groups. Compared with the control groups (ε-PL/SA-0.5 and glass), the number of platelets attached to the coated surface was much less, and the edges of platelets were smooth, indicating that the adhesion platelets are not activated as there are no obvious spurs in the SEM image at high magnifications. However, the two control groups showed many platelets on the surface, and the platelets on the glass surface was proved to be activated with the spurs. Furthermore, Fig. S11 (Supporting Information) showed that less blood composites were deposited on the heparin/YIGSR coated surface compared with uncoated surface and glass surface. The results showed that coaxial-printed ε-PL/SA tubes coated with heparin and YIGSR can effectively prevent platelet adhesion and inhibit platelet activation. The introduction of heparin was designed to protect from thrombosis, and YIGSR was facilitated to cellular attachment, but it proved to EC-specificity adhesion over platelets [33]. Therefore, the introduction of the coating composed of heparin and YIGSR have greatly improved the hemocompatibility of the ε-PL/SA based tubes.

3.5. *Biocompatibility and biofunctionalization of the ε-PL/SA composites with a functional coating*

Development of materials that mimic the structures, properties and functions of natural ECM and enable the study of cells in vitro in a realistic and adaptable cell microenvironment have been an important focus. Herein, heparin and YIGSR was immobilized on the surface of coaxial-printed stable vascular-like tube for regulating the behavior of HUVECs and HPVASMCs. It was identified that heparin could enhance the proliferation of ECs and inhibit migration and proliferation of SMCs [20]. YIGSR is a functional peptide for cellular attachment, and has demonstrated EC-specificity over platelets [33]. In vitro cell biocompatibility was studied by using CCK-8 assay and LIVE/DEAD viability kit and the cell behaviors (such as spreading and sprout) of HUVEC was also observed (Fig. 6). Fig. 6A revealed the viability of HUVECs cultured with samples that coated with 0, 5, 9 heparin/YIGSR coating layers after 3 days. The viability of HUVECs was increased when the coating layers increasing from 0 to 9. For ε-PL/SA-0.25, it showed that the cell viability of uncoated substrate ε-PL/SA (0 heparin/YIGSR coating layers) was much lower than of samples coated with 9 heparin/YIGSR layers. Fig. 6B revealed the viability of HUVECs cultured with samples that coated with 9 heparin/YIGSR layers for 1, 3, 5 days. The cell viability was increased on the ε-PL/SA-0.25-9 when the coating layers increased, and proliferation of HUVECs seeded on the samples were increased significantly from 1st day to 5th day. Additionally, as the ratio of ε-PL to SA was increased from 0.25 to 2, the cell viability was increased. As shown in Fig. 6C and D, the cell viability of HPVASMCs on the samples coated with 9 heparin/YIGSR layers was higher than that uncoated, and with the culturing time increasing, the HPVASMCs were significant increased. As shown in Fig. 6E, the spreading and proliferation of HUVECs cultured for 1 day and 5 days were directly observed and studied by LIVE/DEAD viability kit (the upper row and middle row) and HUVECs cultured for 5 days were also investigated by SEM (the bottom row). After 1 day seeded on the coated samples, HUVECs were attached to the surface. Meanwhile, the cells were spreading more evenly and confluent on the coated ε-PL/SA films after cultured for 5 days compared with cells cultured for 1 day, indicating the favorable tendency of endothelialization for HUVECs on the coated ε-PL/SA films. Furthermore, the cells morphologies on the coated ε-PL/SA films after culture of 5 days were further investigated by SEM (Fig. 6E, the bottom row and Fig. S12, Support Information). It showed that the cells attached on the surface tightly, were confluent with each other which obviously formed polygonal structure and the endothelia sprouts [24], which was accordance with the results from Live/Dead staining. These results revealed that the functional integration of heparin and YIGSR could be improved the endothelialization of the ε-PL/SA tube.

4. Conclusion

In summary, a ε-PL/SA polyelectrolyte-based vascular-like tube with a functional coating of heparin and YIGSR is successfully developed via coaxial printing and electrostatic LbL self-assembly. Due to the electrostatic interactions, the coaxial printed ε-PL/SA tubes can be easily fabricated with tunable diameters, structural integrity as well as facile biofunctionializion. Meanwhile, the functional coating composed of heparin and YIGSR on ε-PL/SA polyelectrolyte-based vascular-like tube was deposited by electrostatic LbL assembly. The sequential release behavior of heparin and YIGSR that heparin was first sustained release at a higher speed than YIGSR and then the release speed of YIGSR was higher than that of heparin could mimic the sequential requirements for antithrombogenicity and endothelialization of small-diameter vascular grafts. Further, the results from cell evaluation in vitro confirmed that the functional coating of heparin and YIGSR not only improved the hemocompatibility and biocompatibility, but also promoted the endotheliazation and angiogenesis of ε-PL/SA polyelectrolyte-based vascular-like tube. This study offers a solid method to coaxially print a small-diameter vascular graft with a biologically inspired release system via the electrostatic interaction, presenting a huge potential for development of small-diameter artificial vascular grafts with good patency.

CRediT authorship contribution statement

Zhiwen Zeng: Investigation, Conceptualization, Data curation, Writing - original draft, Project administration. **Chengshen Hu:** Data curation, Visualization. **Qingfei Liang:** Data curation, Resources. **Lan Tang:** Data curation, Writing - review & editing. **Delin Cheng:** Resources, Visualization, Funding acquisition. **Changshun Ruan:** Conceptualization, Methodology, Writing - original draft, Supervision, Project administration, Funding acquisition.

Declaration of competing interest

We declare that we do not have any commercial or associative interest that represents a conflict of interest in connection with the work submitted.

Acknowledgements

The authors gratefully acknowledge the support for this work from the National Key research and Development Program (Grant No. 2018YFA0703100); the National Natural Science Foundation of China (Grant Nos. 82072082, 31900959); the Youth Innovation Promotion Association of CAS (Grant No. 2019350); the Guangdong Natural Science Foundation (Grant No. 2019A1515011277) and the Shenzhen Fundamental Research Foundation (Grant No. JCYJ20180507182237428).

Appendix A. Supplementary data

Supplementary data to this article can be found online at https://doi.org/10.1016/j.bioactmat.2020.10.028.

References

[1] W. Jiang, D. Rutherford, T. Vuong, H. Liu, Nanomaterials for treating cardiovascular diseases: a review, Bioact Mater. 2 (2017) 185–198.

[2] Y. Wei, Y. Wu, R. Zhao, K. Zhang, A.C. Midgley, D. Kong, Z. Li, Q. Zhao, MSC-derived sEVs enhance patency and inhibit calcification of synthetic vascular grafts by immunomodulation in a rat model of hyperlipidemia, Biomaterials 204 (2019) 13–24.

[3] M. Carrabba, P. Madeddu, Current strategies for the manufacture of small Size tissue engineering vascular grafts, Front. Bioeng. Biotech. 6 (2018) 41.

[4] Q. Gao, Y. He, J.Z. Fu, A. Liu, L. Ma, Coaxial nozzle-assisted 3D bioprinting with built-in microchannels for nutrients delivery, Biomaterials 61 (2015) 203–215.

[5] W. Jia, P.S. Gungor-Ozkerim, Y.S. Zhang, K. Yue, K. Zhu, W. Liu, Q. Pi, B. Byambaa, M.R. Dokmeci, S.R. Shin, A. Khademhosseini, Direct 3D bioprinting of perfusable vascular constructs using a blend bioink, Biomaterials 106 (2016) 58–68.

[6] Y. Zhang, Y. Yu, A. Akkouch, A. Dababneh, F. Dolati, I. Ozbolat, In vitro study of directly bioprinted perfusable vasculature conduits, Biomater. Sci. 3 (2015) 134–143.

[7] Q. Gao, Z. Liu, Z. Lin, J. Qiu, Y. Liu, A. Liu, Y. Wang, M. Xiang, B. Chen, J. Fu, Y. He, 3D bioprinting of vessel-like structures with multilevel fluidic channels, ACS Biomater. Sci. Eng. 3 (2017) 399–408.

[8] S. Hong, J.S. Kim, B. Jung, C. Won, C. Hwang, Coaxial bioprinting of cell-laden vascular constructs using a gelatin-tyramine bioink, Biomater. Sci. 7 (2019) 4578–4587.

[9] I. Holland, J. Logan, J. Shi, C. McCormick, D. Liu, W. Shu, 3D biofabrication for tubular tissue engineering, Bio-Des. Manuf. 1 (2) (2018) 89–100.

[10] Y. Yang, D. Lei, H. Zou, S. Huang, Q. Yang, S. Li, F. Qing, X. Ye, Z. You, Q. Zhao, Hybrid electrospun rapamycin-loaded small-diameter vascular grafts effectively inhibit intimal hyperplasia, Acta Biomater. 97 (2019) 321–332.

[11] N.K. Awad, H. Niu, U. Ali, Y.S. Morsi, T. Lin, Electrospun fibrous scaffolds for small-diameter blood vessels: a review, Membranes 8 (1) (2018) 15.

[12] W. Chen, W. Zeng, Y. Wu, C. Wen, L. Li, G. Liu, L. Shen, M. Yang, J. Tan, C. Zhu, The construction of tissue-engineered blood vessels crosslinked with adenosine-loaded chitosan/beta-cyclodextrin nanoparticles using a layer-by-layer assembly method, Adv. Healthc Mater. 3 (2014) 1776–1781.

[13] Y. Wang, S. Chen, Y. Pan, J. Gao, D. Tang, D. Kong, S. Wang, Rapid in situ endothelialization of a small diameter vascular graft with catalytic nitric oxide generation and promoted endothelial cell adhesion, J. Mater. Chem. B 3 (2015) 9212–9222.

[14] Y. Yang, P. Gao, J. Wang, Q. Tu, L. Bai, K. Xiong, H. Qiu, X. Zhao, M.F. Maitz, H. Wang, X. Li, Q. Zhao, Y. Xiao, N. Huang, Z. Yang, Endothelium-mimicking multifunctional coating modified cardiovascular stents via a stepwise metal-catechol-(amine) surface engineering strategy, Research (2020), 2020 9203906.

[15] T. Yang, Z. Du, H. Qiu, P. Gao, X. Zhao, H. Wang, Q. Tu, K. Xiong, N. Huang, Z. Yang, From surface to bulk modification: plasma polymerization of amine-bearing coating by synergic strategy of biomolecule grafting and nitric oxide loading, Bioact Mater. 5 (2020) 17–25.

[16] Z. Wang, C. Liu, Y. Xiao, X. Gu, Y. Xu, N. Dong, S. Zhang, Q. Qin, J. Wang, Remodeling of a cell-Free vascular graft with nanolamellar intima into a neovessel, ACS Nano 13 (2019) 10576–10586.

[17] W. Gong, D. Lei, S. Li, P. Huang, Q. Qi, Y. Sun, Y. Zhang, Z. Wang, Z. You, X. Ye, Q. Zhao, Hybrid small-diameter vascular grafts: anti-expansion effect of electrospun poly ε-caprolactone on heparin-coated decellularized matrices, Biomaterials 76 (2016) 359–370.

[18] X. Dong, X. Yuan, L. Wang, J. Liu, A.C. Midgley, Z. Wang, K. Wang, J. Liu, M. Zhu, D. Kong, Construction of a bilayered vascular graft with smooth internal surface for improved hemocompatibility and endothelial cell monolayer formation, Biomaterials 181 (2018) 1–14.

[19] P. Gao, H. Qiu, K. Xiong, X. Li, Q. Tu, H. Wang, N. Lyu, X. Chen, N. Huang, Z. Yang, Metal-catechol-(amine) networks for surface synergistic catalytic modi fi cation: therapeutic gas generation and biomolecule grafting, Biomaterials 248 (2020) 119981.

[20] Z. Yang, X. Zhao, R. Hao, Q. Tu, X. Tian, Y. Xiao, K. Xiong, M. Wang, Y. Feng, N. Huang, G. Pan, Bioclickable and mussel adhesive peptide mimics for engineering vascular stent surfaces, Proc. Natl. Acad. Sci. Unit. States Am. 117 (28) (2020) 16127–16137.

[21] W. Du, K. Zhang, S. Zhang, R. Wang, Y. Nie, H. Tao, Z. Han, L. Liang, D. Wang, J. Liu, N. Liu, Z. Han, D. Kong, Q. Zhao, Z. Li, Enhanced proangiogenic potential of mesenchymal stem cell-derived exosomes stimulated by a nitric oxide releasing polymer, Biomaterials 133 (2017) 70–81.

[22] X. Li, J. Liu, T. Yang, H. Qiu, L. Lu, Q. Tu, K. Xiong, N. Huang, Z. Yang, Mussel-inspired "built-up" surface chemistry for combining nitric oxide catalytic and vascular cell selective properties, Biomaterials 241 (2020) 119904.

[23] Z. Lin, M. Wu, H. He, Q. Liang, C. Hu, Z. Zeng, D. Cheng, G. Wang, D. Chen, H. Pan, C. Ruan, 3D printing of mechanically stable calcium-free alginate-based scaffolds with tunable surface charge to enable cell adhesion and facile biofunctionalization, Adv. Funct. Mater. 29 (2019) 1808439.

[24] R. Mammadov, B. Mammadov, S. Toksoz, B. Aydin, R. Yagci, A.B. Tekinay, M. O. Guler, Heparin mimetic peptide nanofibers promote angiogenesis, Biomacromolecules 12 (2011) 3508–3519.

[25] A. Gao, R. Hang, W. Li, W. Zhang, P. Li, G. Wang, L. Bai, X. Yu, H. Wang, L. Tong, P. K. Chu, Linker-free covalent immobilization of heparin, SDF-1alpha, and CD47 on PTFE surface for antithrombogenicity, endothelialization and anti-inflammation, Biomaterials 140 (2017) 201–211.

[26] T.D. Tang, S. Chen, D. Hou, J. Gao, L. Jiang, J. Shi, Q. Liang, D. Kong, S. Wang, Regulation of macrophage polarization and promotion of endothelialization by NO generating and PEG-YIGSR modified vascular graft, Mat. Sci. C-Mater. 84 (2018) 1–11.

[27] T. Ren, S. Yu, Z. Mao, S.E. Moya, L. Han, C. Gao, Complementary density gradient of poly(hydroxyethyl methacrylate) and YIGSR selectively guides migration of endotheliocytes, Biomacromolecules 15 (2014) 2256–2264.

[28] H. Liu, H. Zhou, H. Lan, F. Liu, X. Wang, Multinozzle multichannel temperature deposition system for construction of a blood vessel, SLAS Technol. 23 (2018) 64–69.

[29] H.W. Ooi, C. Mota, A.T. Ten Cate, A. Calore, L. Moroni, M.B. Baker, Thiol-ene alginate hydrogels as versatile bioinks for bioprinting, Biomacromolecules 19 (2018) 3390–3400.

[30] G. Huang, F. Li, X. Zhao, Y. Ma, Y. Li, M. Lin, G. Jin, T.J. Lu, G.M. Genin, F. Xu, Functional and biomimetic materials for engineering of the three-dimensional cell microenvironment, Chem. Rev. 117 (2017), 12764-1285.

[31] D. Radke, W. Jia, D. Sharma, K. Fena, G. Wang, J. Goldman, F. Zhao, Tissue engineering at the blood-contacting surface: a review of challenges and strategies in vascular graft development, Adv. Healthc Mater. 7 (2018), e1701461.

[32] J. Dedic Hio, S. Roke, Polyelectrolytes induce water-water correlations that result in dramatic viscosity changes and nuclear quantum effects, Sci. Adv. 5 (2019), eaay1443.

[33] H.W. Jun, J.L. West, Modification of polyurethaneurea with PEG and YIGSR peptide to enhance endothelialization without platelet adhesion, J. Biomed. Mater. Res. B 72 (2005) 131–139.